Carbon Deposition Properties of $Ni_{0.5}M_{0.5}$/10Sc1CeSZ (M = Cu, Co and Fe) Cermet Anode for Dry Reforming Methane-Fuelled Solid Oxide Fuel Cells

Carbon Deposition Properties of $Ni_{0.5}M_{0.5}$/10Sc1CeSZ (M = Cu, Co and Fe) Cermet Anode for Dry Reforming Methane-Fuelled Solid Oxide Fuel Cells

A A Jais[1], M R Somalu[1,*], A Muchtar[1,2], W N R W Isahak[3]

[1]Fuel Cell Institute, Universiti Kebangsaan Malaysia, UKM Bangi, 43600 Selangor, Malaysia
[2]Centre for Materials Engineering and Smart Manufacturing (MERCU), Faculty of Engineering and Built Environment, Universiti Kebangsaan Malaysia, UKM Bangi, 43600 Selangor, Malaysia
[3]Department of Chemical and Process Engineering, Faculty of Engineering and Built Environment, Universiti Kebangsaan Malaysia, UKM Bangi, 43600 Selangor, Malaysia

*Corresponding author e-mail: mahen@ukm.edu.my

Abstract. Nickel-based cermet anode can be operated in hydrogen and hydrocarbon-fuelled intermediate temperature solid oxide fuel cells (SOFCs). Nickel/zirconia co-doped with 10 mol% scandia and 1 mol% ceria (Ni/10Sc1CeSZ) has better electrochemical performance compared with the state-of-the art SOFC anode, Ni/yttria-stabilised-zirconia. In this study, nickel-metal/10 mol% scandia-1 mol% ceria-stabilised zirconia ($Ni_{0.5}M_{0.5}$/10Sc1CeSZ, M = Co, Cu and Fe) composite anode powders were synthesised via a single-step microwave-assisted glycine nitrate process. The phase identification and morphology of the prepared powder were investigated by X-ray diffraction and field-emission scanning electron microscopy, respectively. The carbon deposition properties of Ni/10Sc1CeSZ and $Ni_{0.5}M_{0.5}$/10Sc1CeSZ (M = Co, Cu and Fe) cermet anode in dry methane fuel were evaluated. Cermet anode powder was reduced under a mixture of hydrogen (10%) and nitrogen (90%) at 800 ℃ for 2 h prior to the carbon deposition test. In the carbon deposition test, the reduced cermet powder was exposed in dry methane atmosphere at 800 ℃ for 3 h. Overall, $Ni_{0.5}Cu_{0.5}$/10Sc1CeSZ cermet anode exhibits the highest intensity ratio of G/D (2.64) in Raman analysis, resulting in less amorphous carbon deposits. This study shows that copper metal substitution could suppress carbon deposition onto Ni/10Sc1CeSZ cermet, and this material can be used as an anode material for SOFCs that operate on dry methane fuel.

1. Introduction

Solid oxide fuel cells (SOFCs) have received considerable attention worldwide as one of the most promising materials for power generation because of low emission, fuel flexibility, absence of noble catalytic metals and high efficiency (55-65 %) [1]. Usually, nickel is used with yttria-stabilised zirconia (YSZ), a ceramic-metallic composite (cermet), as anode material in the SOFC application. Nickel is used because it is inexpensive and provides high catalytic activity for the oxidation of H_2 in SOFCs. Meanwhile, YSZ in the Ni/YSZ cermet plays important roles such as matching the thermal expansion with other components, suppressing grain growth of Ni and providing ionic conductivity.

According to previous report, nickel/scandia-ceria stabilised zirconia (Ni/10Sc1CeSZ) exhibits better electrochemical performance and less carbon deposition than Ni/YSZ [2, 3].

The high operating temperature of SOFCs allows the use of various fuels including hydrocarbon fuel, such as methane. During the internal reforming of methane by Ni/YSZ, the active sites of the Ni anode are covered by the deposited carbon, which results in the deactivation of catalytic activity and decreased cell performance. Existing studies on SOFC anode have focused on alternative anode materials, such as metal-ceramic composites, nickel alloys and perovskite-structured oxides to reduce the carbon deposition problem. Nickel metal in the Ni/YSZ and nickel/gadolinia-doped ceria (Ni/GDC) cermet anodes can be partly or completely replaced by other metals, such as Mn, Co, Cu or Fe, to reduce carbon deposition [4–8].

The properties and performance of cermet anode can be improved by using suitable synthesis techniques. Several powder synthesis methods, such as solid-state reaction [2, 9], sol-gel method [10] and glycine nitrate process (GNP) [11], have been applied for the synthesis of nickel-based (Ni/YSZ, Ni/ScSZ, Ni/GDC) cermet anode materials. Each powder synthesis method has its own advantages and disadvantages. The solution combustion technique is a simple powder synthesis method. It is a self-sustaining combustion process used to produce nanosized ceramic powders with improved shape, size and properties. Microwave energy have been introduced as ignition techniques to initiate combustion synthesis. Enhancement of uniform reaction medium, acceleration of reaction rates and reduction of reaction time were the advantages of microwave application [12–15]. Uniform heating and fast reaction kinetics were generally provided by the microwave energy, which accelerates the reaction rate and increases homogeneity of the final product. While, the heat is transferred to the reactants with slow rate through the vessel walls in conventional heating.

The fundamental study on the carbon deposition properties of Ni/10Sc1CeSZ cermet anode partially substituted by Co, Cu and Fe metals for direct methane fuelled SOFCs has not been well reported till present. Also, the impacts of microwave-assisted combustion method as a new technique on the properties of the anode has not been reported in any studies to the best of author's knowledge. Therefore, in this study, nickel-metal/10 mol% scandia-1 mol% ceria-stabilised zirconia ($Ni_{0.5}M_{0.5}$/10Sc1CeSZ, M = Co, Cu and Fe) composites as anode material were synthesised via a microwave-assisted combustion method. The effects of metal substitution on the carbon deposition behaviour of Ni/10Sc1CeSZ cermet anode were investigated. The composition ratio of 10Sc1CeSZ electrolyte ceramic and metal (nickel or nickel-metal alloy) was 1:1 in vol%, which is based on the percolation theory for nickel metal phase.

2. Experimental procedure

2.1. Preparation of powder

$Ni_{0.5}M_{0.5}O$/10Sc1CeSZ (M = Co, Cu and Fe) composite powders were synthesised through a single-step microwave-assisted GNP (MW-GNP) [13]. Scandium oxide (Sc_2O_3, Aldrich, Germany), nitric acid (HNO_3, Friendemann Schmidt, Australia), cerium(III) nitrate hexahydrate ($Ce(NO_3)_3 \cdot 6H_2O$, Aldrich, Germany), zirconium(IV) oxynitrate hydrate ($ZrO(NO_3)_2 \cdot H_2O$, Acros Organics, Belgium), nickel(II) nitrate hexahydrate ($Ni(NO_3)_2 \cdot 6H_2O$, Friendemann Schmidt, Australia), cobalt(II) nitrate hexahydrate ($Co(NO_3)_2 \cdot 6H_2O$, Merck, Germany), copper(II) nitrate trihydrate ($Cu(NO_3)_2 \cdot 3H_2O$, Sigma-Aldrich, Germany), and iron(III) nitrate nonahydrates ($Fe(NO_3)_3 \cdot 9H_2O$, Friendemann Schmidt, Australia) were used as starting raw materials. Sc_2O_3 was dissolved in a hot HNO_3 solution to form a clear $Sc(NO_3)_2$ solution. Stoichiometric amounts of $ZrO(NO_3)_2 \cdot H_2O$, $Ce(NO_3)_3 \cdot 6H_2O$ and metal nitrates were dissolved in deionised water and added to the prepared $Sc(NO_3)_2$ solution. Glycine ($C_2H_5NO_2$, Genemark, Taiwan) as fuel with a molar ratio of 1:2 of glycine to nitrate was added to the solution and was continuously stirred on the hot plate. The self-combustion of viscous solution was happened in the domestic microwave oven (SHARP, 2450 MHz, 900 W) after the exposure of microwave with 80% of power. Ash was pre-calcined in air at 800 ℃ for 2 h by using a muffle furnace, and composite anode powders with desired composition were obtained. The pre-calcined

composites were further calcined in air at 1300 ℃ for 4 h prior to the evaluation of carbon deposition onto cermet anode powder.

2.2. Characterisation of powder

The phase characterisation of the calcined powder was determined by X-ray diffraction (XRD) from 20 °to 90 °of 2θ by using an X-ray diffractometer (D8-Advance, Bruker, Germany) with a radiation of CuKα (λ = 0.15418 nm). The morphology of calcined powder was examined by Field emission scanning electron microscopy (FESEM; Supra-55VP, Zeiss, Germany).

2.3. Evaluation of carbon deposition

The calcined anode powder was placed on quartz wool pieces in a quartz tube fixed bed reactor. The powder was then reduced in humidified hydrogen gas at 800 ℃ for 2 h and exposed to dry methane gas (ratio CH_4:N_2 = 1:1 in vol%) at 800 ℃ for 3 h, resulting in the deposition of carbon onto the powder from the decomposition of methane gas. Laser Raman spectroscopy of the anode powder was performed after dry CH_4 treatment by using a confocal micro-Raman spectrometer (DXR2xi, Thermo Scientific, USA) with a laser (wavelength = 532 nm) as the excitation source. Thermal gravimetric analysis (TGA; TGA/DSC 1 HT, Mettler Toledo, USA) was conducted from 30 ℃ to 900 ℃ at 20 ℃/min heating rate in air to allow the carbon to be re-oxidised with oxygen. The quantity of deposited carbon was calculated by analysing the weight loss within the temperature range of 500 ℃ to 700 ℃.

3. Results and discussion

The phase of $Ni_{0.5}M_{0.5}O$/10Sc1CeSZ (M = Co, Cu and Fe) anode powder synthesised through single-step MW-GNP was determined based on XRD patterns. Figure 1 shows the phase analysis from the XRD patterns of the anode composite powders. The search and match analysis of the XRD pattern of NiO/10Sc1CeSZ using X'Pert HighScore software revealed two phases of a cubic fluorite-type structure of 10Sc1CeSZ electrolyte and NiO with a Fm-3m (225) space group. No impurities and other phases were observed. The reference file of ZrO2 (96-500-0039) and NiO (96-101-0382) were used for this verification. For bimetallic nickel-metal oxide composites, Co_3O_4 (96-900-5898), CuO (96-901-5825) and Fe_2O_3 (96-900-5817) phases were observed in $Ni_{0.5}M_{0.5}O$/10Sc1CeSZ, $Ni_{0.5}M_{0.5}O$/10Sc1CeSZ and $Ni_{0.5}M_{0.5}O$/10Sc1CeSZ, respectively. The XRD results showed that the metal was unable to be completely substituted in NiO, which is consistent with other reported studies [6, 16]. Even though the sample did not reach complete solubility of metal in NiO, each metal was completely soluble in $Ni_{0.5}M_{0.5}$/10Sc1CeSZ (M = Co, Cu and Fe) cermet anode when the reduction process of nickel-metal oxide to bimetallic nickel-metal alloy was performed.

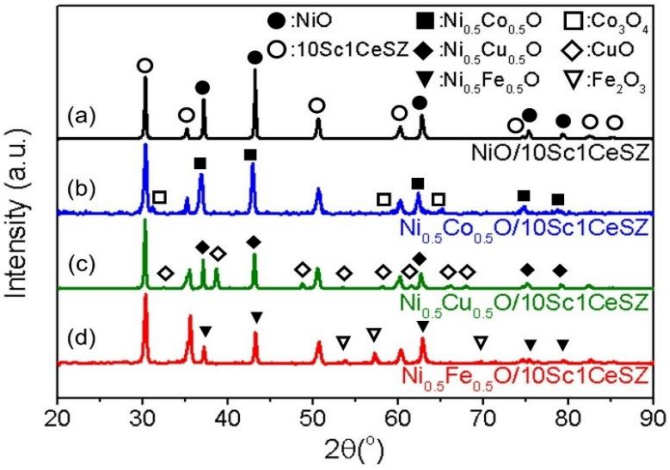

Figure 1 XRD patterns of NiO/10Sc1CeSZ and $Ni_{0.5}M_{0.5}O$/10Sc1CeSZ (M = Co, Cu and Fe) composite powders calcined in air at 800 ℃ for 2 h

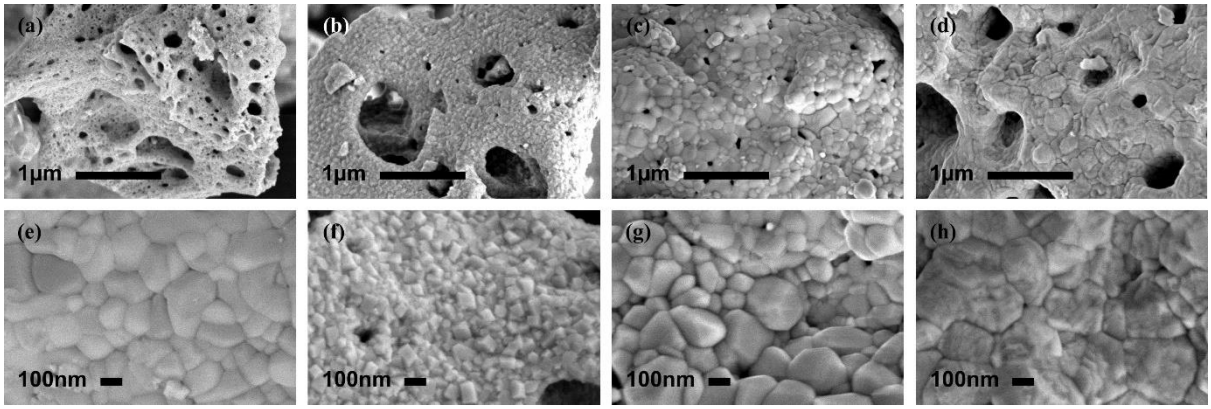

Figure 2 FESEM images of NiO/10Sc1CeSZ (a, e), $Ni_{0.5}Co_{0.5}O$/10Sc1CeSZ (b, f), $Ni_{0.5}Cu_{0.5}O$/10Sc1CeSZ (c, g) and $Ni_{0.5}Fe_{0.5}O$/10Sc1CeSZ (d, h) composite powders calcined at 800 ℃ for 2 h

The particle morphologies of calcined NiO/10Sc1CeSZ and $Ni_{0.5}M_{0.5}O$/10Sc1CeSZ (M = Co, Cu and Fe) anode powder synthesised by MW-GNP combustion method are shown in Figure 2. The calcined anode powder consists of regular shape and homogeneously distributed crystallites. The porous and spongy-shaped-like particles were connected to each other and formed agglomerates [17, 18]. This porosity was formed by the reaction of produced gas that broke out during rapid combustion.

Figure 3 shows the TG profiles of the treated cermet anode in air after exposure in dry CH_4. The amount of carbon deposited onto all cermet powders was calculated from the TGA data. The weight losses at the temperature range of 500 ℃–700 ℃ can be assigned to the reaction of deposited carbon onto carbon dioxide . The observed carbon deposition was most likely the result of CH_4 pyrolysis because the evaluation of carbon deposition behaviour was performed in a dry CH_4 atmosphere in the present study. The formation of carbon at cermet anodes operating on CH_4 oxidation occurs via pyrolysis [19] based on equation (1):

$$CH_4 \rightarrow C + 2H_2 \quad (1)$$

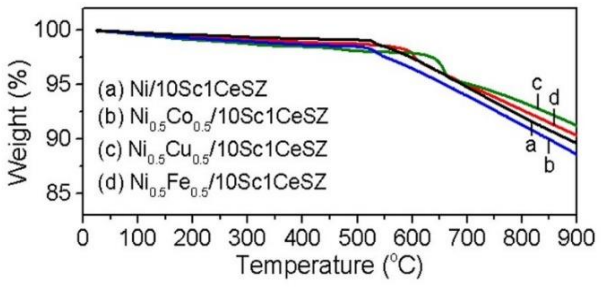

Figure 3 TG result of the reduced Ni/10Sc1CeSZ and $Ni_{0.5}M_{0.5}$/10Sc1CeSZ (M = Co, Cu and Fe) cermet anode after exposure to dry methane gas for 3 h

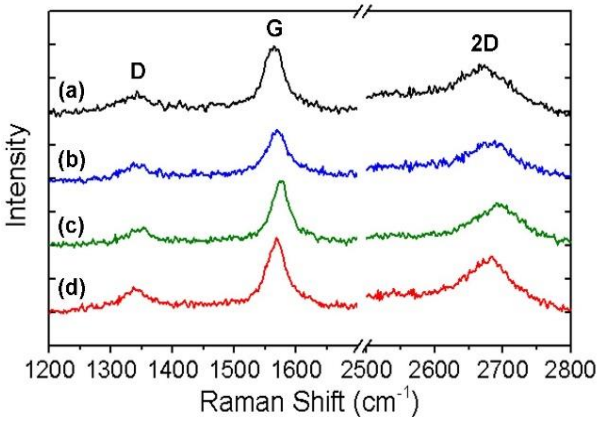

Figure 4 Raman spectra of (a) Ni/10Sc1CeSZ and (b–d) $Ni_{0.5}M_{0.5}$/10Sc1CeSZ (M = Co, Cu and Fe) cermet anode after treatment in dry methane gas for 3 h

The amount of deposited carbon for the $Ni_{0.5}Cu_{0.5}$/10Sc1CeSZ and $Ni_{0.5}Fe_{0.5}$/10Sc1CeSZ cermet decreased compared with the amount of carbon deposited onto the Ni/10Sc1CeSZ cermet. The lowest amount of carbon was deposited onto $Ni_{0.5}Cu_{0.5}$/10Sc1CeSZ. Meanwhile, $Ni_{0.5}Co_{0.5}O$/10Sc1CeSZ cermet exhibited approximately similar amount of deposited carbon with Ni/10Sc1CeSZ cermet. These results show that metal copper substitution can suppress carbon formation on the surface of Ni/10Sc1CeSZ cermet anode.

Figure 4 shows the Raman spectra of the cermet anode after exposure to dry methane atmosphere. Raman spectra were analysed to investigate the deposited carbon structures on the cermet anode treated in dry methane. Three intense peaks assigned to the defect (D), graphite (G) and 2D bands of carbon at the Raman shift range of 1342–1353, 1563–1572 and 2664–2690 cm^{-1} were observed, respectively. The intensity of G band was higher than that of D band for all treated cermet anodes. The G band, which is the main fundamental peak, corresponds to the crystalline structure of graphitic layer and carbon atom vibration. The D band is related to disorder of the carbon structure, whilst the 2D band occurs from a resonant interaction of incident light with the electronic structure of the carbon [10, 20]. The graphitisation degree of carbon is usually represented by the intensity ratio of G/D and is reported to have an approximate value of 0.9 and higher. The calculated intensity ratios of G/D value were consistent at 2.10, 2.14, 2.64 and 2.40 for Ni/10Sc1CeSZ, $Ni_{0.5}Co_{0.5}$/10Sc1CeSZ, $Ni_{0.5}Cu_{0.5}$/10Sc1CeSZ and $Ni_{0.5}Fe_{0.5}$/10Sc1CeSZ treated in dry methane at 800 ℃, respectively. The high graphitisation degree led to less formation of amorphous carbon deposits onto the cermet anode. Amorphous carbon could deactivate the catalytic activity of nickel cermet anode.

Table 1 Amount of carbon deposits in percentage and the intensity ratio of G/D of cermet anode that was exposed to dry methane at 800 ℃ for 3 h.

Cermet anode	Amount of carbon deposits (%)	Intensity ratio of G/D
Ni/10Sc1CeSZ	4.34	2.099
$Ni_{0.5}Co_{0.5}$/10Sc1CeSZ	4.52	2.136
$Ni_{0.5}Cu_{0.5}$/10Sc1CeSZ	3.02	2.635
$Ni_{0.5}Fe_{0.5}$/10Sc1CeSZ	3.75	2.393

The amount of deposited carbon onto cermet anode and the calculated intensity ratio of G/D are summarised in Table 1. These results show that copper metal substitution could suppress carbon deposition onto the Ni/10Sc1CeSZ cermet, and this material is suitable as an anode material for hydrocarbon-fuelled SOFCs. $Ni_{0.5}Cu_{0.5}$/10Sc1CeSZ cermet anode exhibits less amount of carbon deposits after treatment in methane gas for 3 h at 800 ℃ indicating that the cermet anode is suitable to be operated in direct methane fuelled SOFC compared to Ni/10Sc1CeSZ. The deactivation of cermet anode performance by the higher amount of deposited carbons could decreased the performance of SOFC especially when it is operated in direct methane fuel. The information obtained from these results could help to solve the carbon deposition problem and to choose the suitable cermet anode for direct methane SOFC application. In future work, electrochemical impedance spectroscopy measurement and current-voltage characterisation of single cells consisting of $Ni_{0.5}M_{0.5}$/10Sc1CeSZ (M = Co, Cu and Fe) cermet anode will be evaluated for hydrogen and methane fuels.

4. Conclusion

$Ni_{0.5}M_{0.5}$/10Sc1CeSZ (M = Co, Cu and Fe) cermet anode materials were successfully synthesised through single-step MW-GNP. The evaluation of carbon deposition onto the prepared cermet anode was analysed through the results from thermal gravimetry analysis and Raman spectra. The less amount of carbon deposits calculated from TG results was related to the intensity ratio of G/D in Raman spectra. The intensity ratio of G/D for $Ni_{0.5}Cu_{0.5}$/10Sc1CeSZ and $Ni_{0.5}Fe_{0.5}$/10Sc1CeSZ was 2.64 and 2.40, respectively. $Ni_{0.5}Cu_{0.5}$/10Sc1CeSZ exhibits the highest intensity ratio of G/D and resulting to less amount of carbon deposits (3.02%) onto Ni/10Sc1CeSZ cermet anode. The partial substitution of copper and iron metal can suppress the carbon deposition onto the Ni/10Sc1CeSZ

cermet anode. Overall, Cu metal was effective in reducing the amount of carbon deposits onto Ni-based cermet anode and improved the performance of Ni/10Sc1CeSZ cermet anode for direct methane-fuelled SOFC.

Acknowledgment
This work was supported by Universiti Kebangsaan Malaysia (UKM; Grant No. GUP-2018-040). The authors would like to acknowledge the Centre for Research and Instrumentation Management, UKM and Institute of Advanced Technology, Universiti Putra Malaysia for providing excellent testing equipment. The first author gratefully acknowledges Universiti Malaysia Pahang and Ministry of Education Malaysia for a PhD scholarship.

References
[1] Hui S R, Roller J, Yick S, Zhang X, Deces-Petit C, Xie Y, Maric R and Ghosh D 2007 *Journal of Power Sources* **172** 493–502
[2] Somalu M R, Yufit V, Cumming D, Lorente E and Brandon N 2011 *International Journal of Hydrogen Energy* **36** 5557–66
[3] Arifin N, Button T and Steinberger-Wilckens R 2017 *ECS Transactions* **78** 1417–25
[4] Miyake M, Matsumoto S, Iwami M, Nishimoto S and Kameshima Y 2016 *International Journal of Hydrogen Energy* **41** 13625–31
[5] Miyake M, Matsumoto S, Nishimoto S and Kameshima Y 2017 *Journal of the Ceramic Society of Japan* **125** 833–6
[6] Cho C K and Lee K T 2013 *Journal of Ceramic Processing Research* **14** 59–64
[7] Ding G, Gan T, Yu J, Li P, Yao X, Hou N, Fan L, Zhao Y and Li Y 2017 *Catalysis Today* **298** 250–7
[8] Ding H, Tao Z, Liu S and Yang Y 2016 *Journal of Power Sources* **327** 573–9
[9] Baity P S N, Budiana B and Suasmoro S 2017 *IOP Conference Series: Materials Science and Engineering* **214** 012029
[10] Hua B, Li M, Chi B and Jian L 2014 *Journal of Materials Chemistry A* **2** 1150–8
[11] Zhu H, Wang W, Ran R, Su C, Shi H and Shao Z 2012 *International Journal of Hydrogen Energy* **37** 9801–8
[12] Shaikh S P, Somalu M R and Muchtar A 2016 *Journal of Physics and Chemistry of Solids* **98** 91–9
[13] Jais A A, Muhammed Ali S A, Anwar M, Somalu M R, Muchtar A, Isahak W N R W, Tan C Y, Singh R and Brandon N P 2017 *Ceramics International* **43** 8119–25
[14] Ao H, Liu X, Zhang H, Zhou J, Huang X, Feng Z and Xu H 2015 *Journal of Rare Earths* **33** 746–51
[15] Muhammed Ali S A, Anwar M, Somalu M R and Muchtar A 2017 *Ceramics International* **43** 4647–54
[16] Cho C K, Choi B H and Lee K T 2012 *Journal of Alloys and Compounds* **541** 433–9
[17] Pudukudy M, Yaakob Z and Takriff M S 2016 *RSC Advances* **6** 68081–91
[18] Gómez-Romero P, Fraile J and Ballesteros B 2013 *RSC Advances* **3** 2351–4
[19] Cho C K, Choi B H and Lee K T 2013 *Ceramics International* **39** 389–94
[20] Guo Y, Wan T, Zhu A, Shi T, Zhang G, Wang C, Yu H and Shao Z 2017 *RSC Advances* **7** 44319–25